Biochemical and Biophysical Research Communications 409 (2011) 34–39

Contents lists available at ScienceDirect

Biochemical and Biophysical Research Communications

journal homepage: www.elsevier.com/locate/ybbrc

Insulin receptor mutation results in insulin resistance and hyperinsulinemia but does not exacerbate Alzheimer's-like phenotypes in mice

Kazuma Murakami [a,b,1], Shin-ichi Yokoyama [a], Nakaba Murata [a,c], Yusuke Ozawa [a], Kazuhiro Irie [b], Takuji Shirasawa [d], Takahiko Shimizu [a,c,*]

[a] Molecular Gerontology, Tokyo Metropolitan Institute of Gerontology, Itabashi-ku, Tokyo 173-0015, Japan
[b] Division of Food Science and Biotechnology, Graduate School of Agriculture, Kyoto University, Kyoto 606-8502, Japan
[c] Applied Biological Chemistry, United Graduate School of Agricultural Science, Tokyo University of Agriculture and Technology, Fuchu-shi, Tokyo 183-8509, Japan
[d] Department of Aging Control Medicine, Juntendo University Graduate School of Medicine, Bunkyo-ku, Tokyo 113-0033, Japan

ARTICLE INFO

Article history:
Received 20 April 2011
Available online 28 April 2011

Keywords:
Insulin resistance
Hyperinsulinemia
Insulin signaling
Alzheimer's disease
Amyloid β
Senile plaque

ABSTRACT

Obesity is a risk factor for Alzheimer's disease (AD), which is characterized by amyloid β depositions and cognitive dysfunction. Although insulin resistance is one of the phenotypes of obesity, its deleterious effects on AD progression remain to be fully elucidated. We previously reported that the suppression of insulin signaling in a mouse with a heterozygous mutation (P1195L) in the gene for the insulin receptor showed insulin resistance and hyperinsulinemia but did not develop diabetes mellitus [15]. Here, we generated a novel AD mouse model carrying the same insulin receptor mutation and showed that the combination of insulin resistance and hyperinsulinemia did not accelerate plaque formation or memory abnormalities in these mice. Interestingly, the insulin receptor mutation reduced oxidative damage in the brains of the AD mice. These findings suggest that insulin resistance is not always involved in the pathogenesis of AD.

© 2011 Elsevier Inc. All rights reserved.

1. Introduction

Alzheimer's disease (AD) is generally characterized by amyloid deposition in senile plaques mainly consisting of 40- and 42-mer amyloid β-proteins (Aβ40, Aβ42) [1,2]. These proteins are produced from amyloid precursor protein (APP) by two proteases (β- and γ-secretase). Since Aβ42 shows a stronger aggregative ability and neurotoxicity than Aβ40, Aβ42 is considered to play a more important role in the pathogenesis of AD [3]. There is a growing body of evidence that the meta-stable oligomer of Aβ causes synaptic dysfunction and memory impairment in AD [4], whereas mature plaques are believed to be much less active [5] and to serve as a stock for the toxic Aβ aggregates [6]. In addition, the neurotoxicity of Aβ is known to originate from its radicalization or the generation of toxic radical species (e.g., superoxide radicals, hydrogen peroxide, and hydroxyl radicals) by copper and zinc metals [7,8].

Obesity is a risk factor for AD as well as metabolic syndrome including diabetes mellitus, which induces lipid accumulation [9]. Insulin regulates glucose intake from the blood to tissues (e.g., the liver, muscle, and brain) through insulin receptor (IR)-mediated signal transduction [10]. When insulin signaling is disturbed by obesity (we call this "insulin resistance"), the secretion of insulin into the blood is increased in order to transmit insulin signals to nuclei, resulting in hyperinsulinemia. In addition, epidemiological studies have suggested that insulin signaling is impaired in AD patients [11,12]. Townsend et al. reported that soluble Aβ oligomer interferes with insulin-induced autophosphorylation through its binding to IR [13]. The expression of insulin-degrading enzyme is stimulated by insulin signaling in order to degrade Aβ [14]. These findings imply a role for insulin signaling in Aβ aggregation and clearance and suggest that insulin resistance contributes to AD progression. However, little is known about the deleterious effects of insulin resistance on the pathologies of AD *in vivo*. Our group previously reported that a mouse carrying a mutation in the IR ($Ir^{P1195L/wt}$) displayed insulin resistance [15]. $Ir^{P1195L/wt}$ mice, in which insulin signaling is suppressed, develop hyperinsulinemia without diabetes mellitus as they age. Information on the effects of insulin resistance on AD progression is required to elucidate the involvement of insulin signaling in AD.

Therefore, we crossed an $Ir^{P1195L/wt}$ mouse with a human APP (*hAPP*) transgenic mouse (line J20), a well-established AD model [16], to generate a novel double mutant mouse ($hAPP/Ir^{P1195L/wt}$) and analyzed it for AD-like pathology. This report shows that the combination of insulin resistance and hyperinsulinemia does not

* Corresponding author at: Molecular Gerontology, Tokyo Metropolitan Institute of Gerontology, 35-2 Sakae-cho, Itabashi-ku, Tokyo 173-0015, Japan. Fax: +81 3 3579 4776.
E-mail address: shimizut@tmig.or.jp (T. Shimizu).
[1] Research Fellow of the Japan Society for the Promotion of Science.

0006-291X/$ - see front matter © 2011 Elsevier Inc. All rights reserved.
doi:10.1016/j.bbrc.2011.04.101

exacerbate plaque formation, Aβ metabolism, or cognitive impairment in AD mice. Notably, the IR mutation reduced the oxidative damage in the brains of the AD mice. Here, we discuss the biological significance of insulin signaling in AD-like pathologies *in vivo*.

2. Materials and methods

2.1. Animals

Heterozygous transgenic mice; i.e., AD mice (line J20; The Jackson Laboratory), which possess a human APP gene with Swedish (670/671KM->NL) and Indiana (717V->F) mutations driven by the platelet-derived growth factor promoter on a C57BL/6J background, were used [16]. The *hAPP* mice were genotyped by PCR using genomic DNA isolated from the tail tip, as described previously [17,18]. Heterozygous IR mutant mice, $Ir^{P1195L/wt}$ mice [15], that had been maintained in our laboratory were backcrossed with C57BL/6CrSlc mice (Japan SLC, Shizuoka, Japan) for 5 or 6 generations. The genotyping of the $Ir^{P1195L/wt}$ mice was also performed by PCR using genomic DNA isolated from the tail tip, as described elsewhere [15]. The primers for identifying the $Ir^{P1195L/wt}$ genotype, 5′-CAC CTG TTC ATT AGA CAG GCC-3′ and 5′-GGA ATG ACA AGG GAC ATC TA-3′, were used under the following conditions: 1 cycle of 85 °C for 3 min; 94 °C for 90 s; and 30 cycles of 94 °C for 30 s, 53.7 °C for 30 s, and 72 °C for 120 s, followed by 1 cycle of 72 °C for 5 min. Non-*hAPP* $Ir^{wt/wt}$ (wild-type) mice were used as littermate controls.

The animals had *ad libitum* access to water and autoclaved standard chow (CRF-1, Oriental Yeast, Tokyo, Japan). All mice were maintained and studied according to the protocols approved by the Animal Care Committee of Tokyo Metropolitan Institute of Gerontology. In all experiments except for the behavioral tests, the male mice were sequentially subjected to three mazes (the Y-maze, elevated plus maze, and Morris water maze), followed by an analysis of AD-related neuropathology. One brain hemisphere was fixed in 4% paraformaldehyde for 3–5 days for the histological studies, and the opposite hemisphere was rapidly frozen in liquid nitrogen and stored at −80 °C until the biochemical studies.

2.2. Blood analysis

Plasma glucose levels were determined in fasting mice (12 months old) using the ELISA-based Glucose CII-Test (Wako, Osaka, Japan). Plasma insulin levels were measured in fasting mice at the age of 12 months using a mouse insulin ELISA kit (Shibayagi, Gunma, Japan). The absorbance at 505 or 420 nm was estimated using a tunable microplate reader (VersaMax, Molecular Devices).

2.3. Immunohistochemistry

The brain sections (5 μm) were prepared as described previously [17,18]. In brief, anti-Aβ antibody (4G8, 1/1000; Covance Laboratories) was used as the primary antibody. Staining images were acquired with a VS-100 Photomicroscope Unit (Olympus, Tokyo, Japan), and the immunoreactive area was quantified using the Leica Qwin V3 software (Leica Microsystems, Wetzlar, Germany).

2.4. Aβ ELISA

Brain homogenates of the Tris-buffered saline (TBS)-soluble fraction or TBS-insoluble fraction (6 M guanidine-HCl-soluble) were prepared as described previously [17,18]. The total protein concentrations in the brain were determined using the DC protein assay kit (Bio-Rad Laboratories, Hercules, CA, USA). The brain Aβ40 and Aβ42 levels in the TBS-soluble and TBS-insoluble fractions were measured using the sandwich enzyme-linked immunosorbent assay (ELISA) with a human β Amyloid ELISA Kit [Aβ40: Cat# 27714, human amyloid β (1-40)(N); Aβ42: Cat# 27712, human amyloid β (1-42)(N)] (Immuno Biochemical Laboratories, Gunma, Japan) according to the manufacturer's instructions.

2.5. Y-maze

Exploratory behavior was tested using the Y-maze task, as described previously [17,18]. In brief, the mice were placed alone into one arm of the Y-maze apparatus (Muromachi Kikai, Tokyo, Japan) and allowed to explore the maze for 6 min. Each mouse's performance (number of entries into each arm) was monitored with the CompACT VAS/DV video-tracking system (Muromachi Kikai).

2.6. Elevated plus maze

Anxiety was assessed using the elevated plus maze task, as described previously [17,18]. Briefly, in the elevated plus maze apparatus (Muromachi Kikai), the mice were placed alone in the central square of the maze facing one of the open arms and allowed to explore the open and closed arms freely for 10 min. The total time spent in each arm was recorded automatically with the CompACT VAS/DV video-tracking system (Muromachi Kikai).

2.7. Morris water maze

Memory impairment was assessed using the Morris water maze test, as described previously [18,19]. Briefly, in the training phase using the water maze pool (Muromachi Kikai), the mice underwent two daily trials, which were 2 h apart and lasted for 60 s, on 6 consecutive days. The location of the platform remained constant throughout the training phase, but the drop location was changed semi-randomly between trials. On day 7, the platform was removed for a probe trial, and the mice were allowed to swim in the pool for 60 s. Escape latency, the percentage of time spent in each quadrant, and swimming distance were recorded with the CompACT VAS/DV video-tracking system (Muromachi Kikai).

2.8. Dot blot

TBS-soluble fractions (2 μg/μL) treated with 12% SDS were diluted 40-fold with TBS and then applied to a PVDF membrane (0.45 μm pore size, Millipore). After being blocked, the membrane was incubated with anti-CML antibody (1/400, Cosmo Bio, Tokyo) overnight at 4 °C, before being incubated with the secondary antibody (1 h, room temperature). Development was performed with enhanced chemiluminescence and quantified using LAS-4000 (Fujifilm).

2.9. OxyBlot for protein carbonylation

Protein carbonyls were measured using the OxyBlot protein oxidation detection kit (Millipore) according to the manufacturer's instructions. Five microliter samples (2 μg/μL) from the TBS-soluble fraction were treated with 2,4-dinitrophenylhydrazine and applied to PVDF membranes.

2.10. Data analysis

All data are shown as the mean ± SEM, and differences were analyzed with repeated-measures analysis of variance (ANOVA) and the Tukey–Kramer test. $P < 0.05$ was considered significant.

3. Results

3.1. Lifespan and glucose metabolism of the hAPP/$Ir^{P1195L/wt}$ mice

We crossbred J20 mice with mice expressing a mutant IR (P1195L/$Ir^{P1195L/wt}$) to generate double transgenic mice (*hAPP*/$Ir^{P1195L/wt}$). The *hAPP*/$Ir^{P1195L/wt}$ mutant mice were born at frequencies slightly lower than the expected Mendelian ratio in females (19.6%) and males (20.8%), but grew without morphological abnormalities. Kaplan–Meier survival curves showed that the female $Ir^{P1195L/wt}$, *hAPP*, and *hAPP*/$Ir^{P1195L/wt}$ mice displayed 10%, 23%, and 14% lethality at the age of 12 months, respectively (Fig. 1A). On the other hand, all male wild-type, *hAPP*, and *hAPP*/$Ir^{P1195L/wt}$ mice showed 10% lethality at the age of 6 months, and thereafter, no death was observed in any of the groups (Fig. 1B). Statistical analysis showed that the difference in survival rates among these groups was not significant. These findings suggest that IR mutation does not significantly shorten the lifespan of *hAPP* mice. In the female mice, all mouse groups exhibited a similar pattern of body weight increase (Supplementary Fig. S1A), whereas only the male double mutant mice showed a lower body weight than the wild-type mice (Supplementary Fig. S1B).

The gender difference in the glucose metabolism of $Ir^{P1195L/wt}$ mice was previously reported and attributed to endogenous estrogen [15]. Meanwhile, the J20 line of *hAPP* mice did not show any gender differences in glucose metabolism [16], unlike other AD mouse models (e.g., Tg2576 [20]). To investigate whether gender affects the glucose metabolism of *hAPP*/$Ir^{P1195L/wt}$ mice, we measured the plasma glucose and insulin levels of fasting mice using ELISA tests. As shown in Fig. 1C, almost no difference in blood glucose was observed among the four genotypes in either sex. Only the male *hAPP*/$Ir^{P1195L/wt}$ mice developed hyperinsulinemia, but not hyperglycemia, similar to the $Ir^{P1195L/wt}$ mice, and no significant gender difference was found in the plasma insulin level of the *hAPP*/$Ir^{P1195L/wt}$ mice (Fig. 1D). The hyperinsulinemia of the male $Ir^{P1195L/wt}$ mice was consistent with that described in our previous studies [15]; therefore, the subsequent studies of Aβ-related biochemistry were performed using the male mice.

3.2. Insulin resistance does not increase plaque formation or the Aβ content of hAPP mice

We performed immunohistochemistry to assess the level of amyloid plaque deposition in brain sections from the mice including sections of the cortex and hippocampus using anti-Aβ antibody. As shown in Fig. 2A and B, IR mutation (P1195L) reduced the area of Aβ deposition in the 12-month-old *hAPP* mice (2.3 ± 0.4% versus 1.1 ± 0.2%, $p = 0.048$). No plaques were observed in the brains of the wild-type or $Ir^{P1195L/wt}$ mouse groups (Supplementary Fig. S2).

To examine the effect of insulin resistance on the Aβ content of the insoluble and soluble brain fractions, ELISA experiments were carried out. Unexpectedly, the mutation did not increase the amount of insoluble Aβ42 or Aβ40 in the *hAPP* mice (Fig. 2C). These findings imply that the mutation affects Aβ aggregation, but not the amount of Aβ42 or Aβ40 in the brain. Moreover, no changes were observed in the amounts of either Aβ in the soluble fraction although the level of soluble Aβ40 was moderately decreased ($p = 0.053$) (Fig. 2D). These findings indicate that insulin resistance does not accelerate plaque formation or increase the amount of Aβ in the brain.

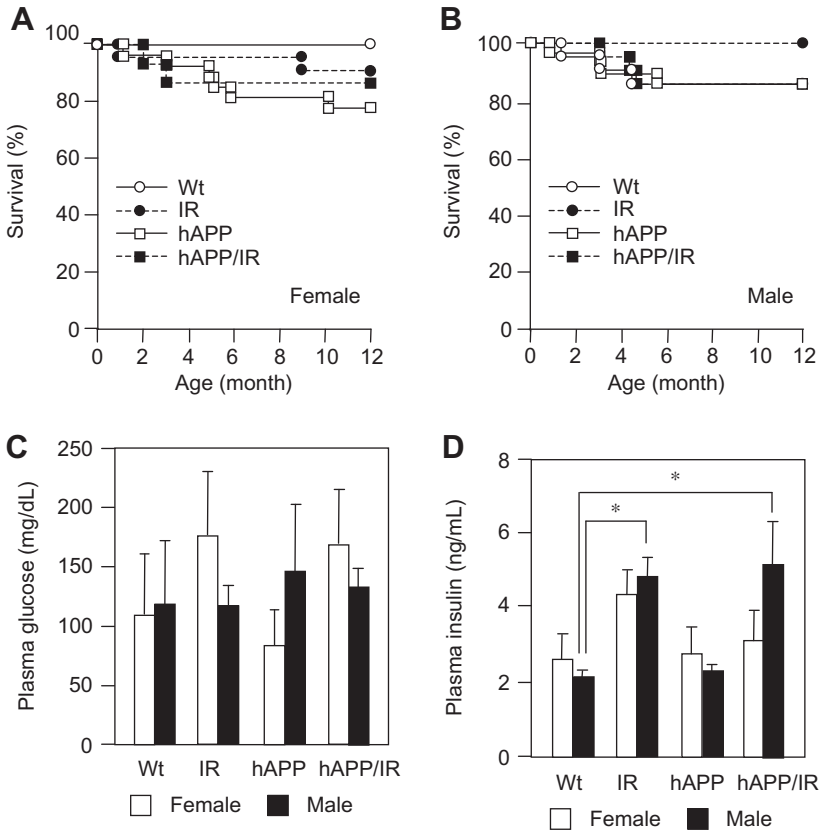

Fig. 1. Lifespan and glucose metabolism of *hAPP*/$Ir^{P1195L/wt}$ mice. (A and B) Kaplan–Meier survival curves of (A) female and (B) male WT (wild-type) ($n = 25$ for females and 23 for males), IR ($Ir^{P1195L/wt}$) ($n = 22$ for females and 34 for males), *hAPP* ($n = 27$ for females and 30 for males), and *hAPP*/$Ir^{P1195L/wt}$ mice ($n = 15$ for females and 23 for males). (C) The plasma glucose and (D) plasma insulin levels of the fasting mice at the age of 12 months ($n = 3$ per genotype/sex). $^*P < 0.05$.

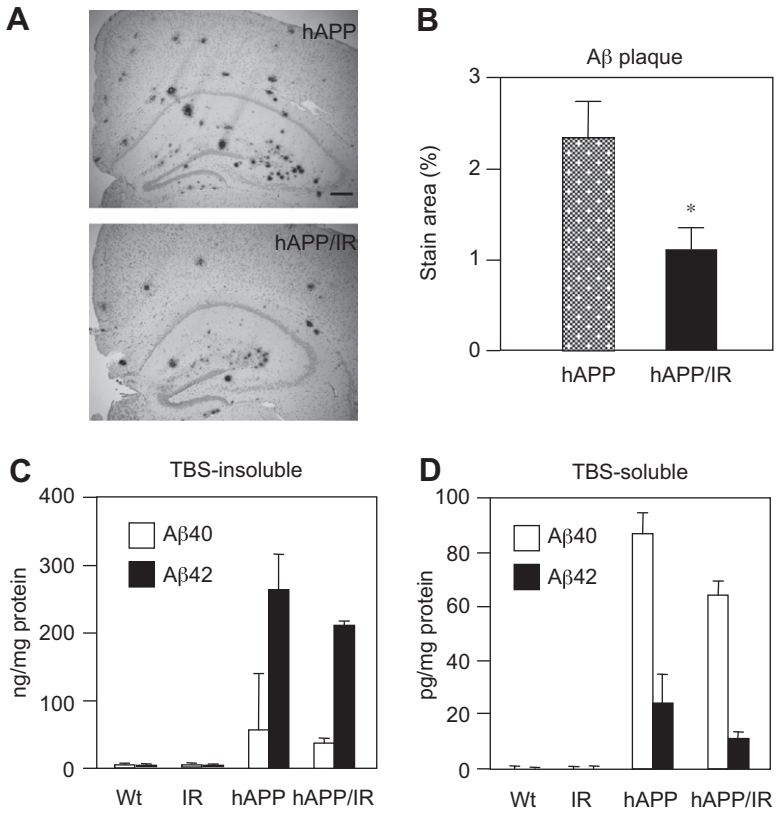

Fig. 2. Insulin resistance does not increase the Aβ plaque burden or Aβ content in 12-month-old male *hAPP* mice. (A) Representative image of amyloid deposits immunostained with 4G8 (anti-Aβ) antibody in 12-month-old *hAPP* mice. The scale bar represents 200 μm. (B) Quantification of the 4G8-positive plaque area (% of section ± SEM) in the cortices and hippocampi of brains from each type of mouse ($n = 4$ per genotype). (C and D) ELISA of (C) TBS-insoluble or (D) TBS-soluble fraction for Aβ40 and Aβ42 ($n = 3$ for WT, 3 for IR, 8 for *hAPP*, and 6 for *hAPP*/$Ir^{P1195L/wt}$ mice). $^*P < 0.05$.

3.3. Insulin resistance does not alter the behavioral abnormalities of *hAPP* mice

AD model mice show behavioral abnormalities (e.g., hyperactivity) related to AD progression, which are independent of gender [21]. In groups of sex-balanced females and males, the *hAPP* mice showed significant hyperactivity characterized by an increased number of total arm entries compared with the wild-type or $Ir^{P1195L/wt}$ mice in the Y-maze test (Fig. 3A). The insulin resistance mutation failed to disturb the hyperactivity of the AD mice. *hAPP* mice also exhibit an altered anxiety and fear phenotype in the elevated plus maze [21]. Although the *hAPP* mice stayed in the closed arms of the elevated plus maze for a shorter period than the wild-type, the mutation did not shorten the time they spent in the closed arms (Fig. 3B). Moreover, the memory loss (escape latency in the training trial and the percentage of time spent in each quadrant in the probe trial) of the *hAPP* mice was not altered by the mutation in the Morris water maze (Fig. 3C and D). The swimming distance of the mice in the probe trial did not differ among the genotypes (data not shown). These findings imply that the insulin resistance induced by the IR mutation did not modulate the behavioral impairment conveyed by the *hAPP* gene.

3.4. Insulin resistance reduced the oxidative damage in the brains of the hAPP mice

Oxidative stress is a well-studied early response in the pathogenesis of AD and other neurodegenerative diseases [7]. Protein oxidation occurs following the reaction of carbonyl groups and amino acid residues (e.g., lysine, arginine, and cysteine) with carbohydrates, leading to the formation of advanced glycation end-products (AGE). The N_ε-carboxymethyl lysine (CML) in AGE is thought to be a critical marker of oxidative damage [22]. To examine the effect of the P1195L mutation on oxidative stress in the brains of *hAPP* mice, two types of dot blots (for CML derivatization and protein carbonylation) were performed. As shown in Fig. 4A, the amount of CML was increased by 31% in the *hAPP* mice compared with that in the wild-type, while the P1195L mutation significantly decreased the CML content of their brains. Regarding the protein carbonyl formation, carbonylation was attenuated by 25% in the *hAPP*/$Ir^{P1195L/wt}$ mice compared with the *hAPP* mice (Fig. 4B). As $Ir^{P1195L/wt}$ mice display increased manganese superoxide dismutase (Mn-SOD) activity [15], which is localized in the mitochondrial matrix and catalyzes the conversion of superoxide radicals to hydrogen peroxide, these mechanisms might be involved in the antioxidant defense conveyed by the P1195L IR mutation.

4. Discussion

$Ir^{P1195L/wt}$ mice display insulin resistance and hyperinsulinemia, but not hyperglycemia [15]. The hyperinsulinemia associated with diabetes mellitus is closely related to the pathogenesis of AD [23]. Contrary to our expectations, the *hAPP*/$Ir^{P1195L/wt}$ mice did not display exacerbated Aβ-related neuropathologies (Fig. 2), behavioral abnormalities (Fig. 3), or oxidative damage (Fig. 4) compared with the AD mouse model. The results of the three maze tests (Fig. 3) performed in this study agreed with the absence of an effect on the level of soluble Aβ assemblies (Fig. 2D), which are responsible for the cognitive decline seen in AD patients [4]. Surprisingly, no

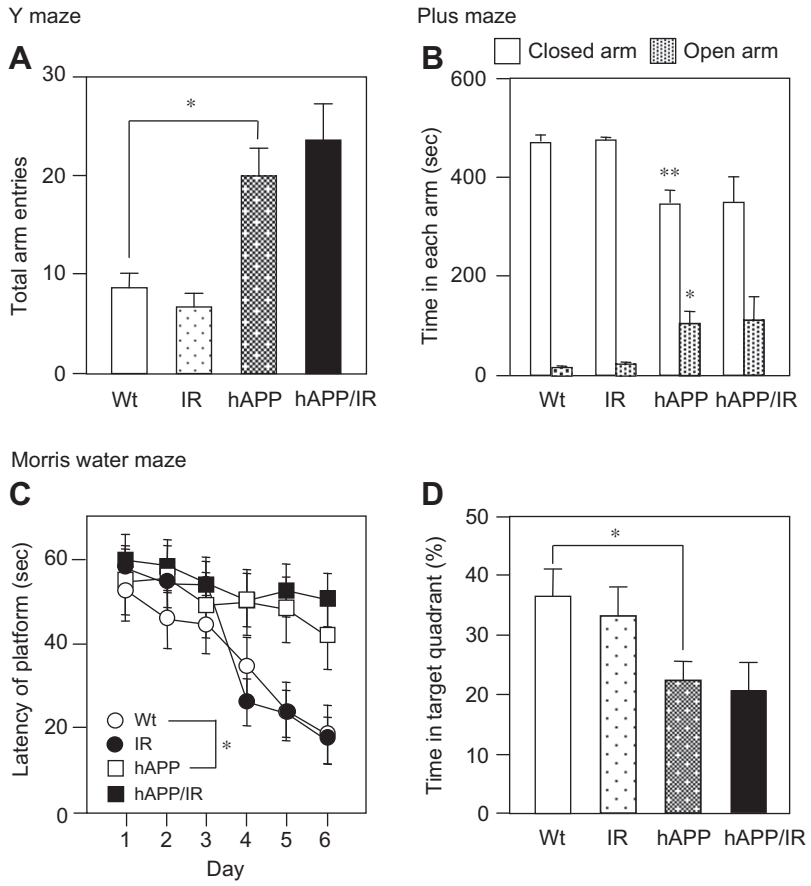

Fig. 3. Insulin resistance does not accelerate the behavioral abnormalities of 10–12-month-old *hAPP* mice. (A) Total arm entries were counted for 6 min in the Y-maze. (B) The percentage of time spent in the open and closed arms during 10 min exploration of the elevated plus maze. (C and D) Morris water maze. (C) The escape latency of the mice during the hidden platform training for a total period of 6 days. (D) Percentage of search time spent in the target quadrant during a 60 s probe trial on day 7. $n = 20$ for the WT, 20 for the IR, 20 for the *hAPP*, and 11 for the *hAPP*/$Ir^{P1195L/wt}$ mice. $^{*}P < 0.05$, $^{**}P < 0.01$.

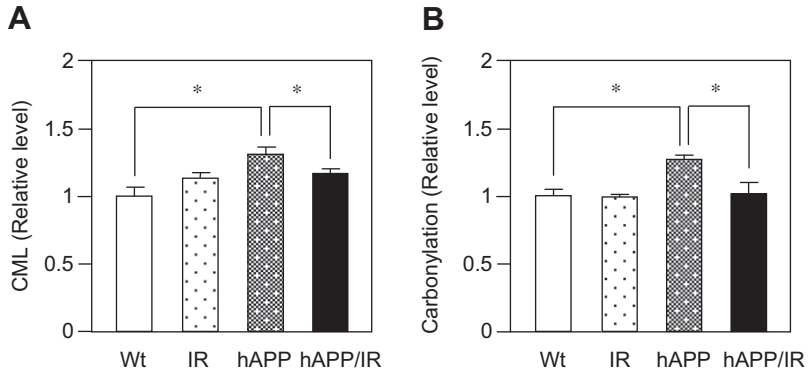

Fig. 4. Insulin resistance prevents oxidative damage in 12-month-old male *hAPP* mice. The densitometric quantification of dot blots of (A) N_{ε}-carboxymethyl lysine (CML) and (B) protein carbonylation in mouse brains ($n = 5$ per genotype). $^{*}P < 0.05$.

change in oxidative damage was observed in the $Ir^{P1195L/wt}$ mice (Fig. 4) in spite of their enhanced Mn-SOD activity [15]. Taken together, we have demonstrated that the P1195L mutation leads to insulin resistance, but does not accelerate AD-like pathologies *in vivo*.

On the other hand, the $Ir^{P1195L/wt}$ mouse is a homologous rodent model that possesses IR similar to the *daf*-2 mutant [15], a longevity mutant that was originally found in the *daf*-2 gene of *Caenorhabditis elegans* [24]. Kimura et al. discovered the *daf*-2 mutant and reported that it induces defective insulin/insulin-like signaling, which extends the survival of *C. elegans* via dauer formation [24]. Hekimi and Guarente suggested that calorie restriction regulates insulin signaling, which in turn alters metabolism to promote the lifespan of organisms ranging from yeast to mammals [25]. Catalase and Mn-SOD also play important roles in extending life duration by acting as antioxidants in response to downregulated insulin-like signaling in *drosophila* [26] and *C. elegans* [27]. Although decreased oxidative stress (Fig. 4) might contribute to the suppression of senile plaque formation by eliminating the radical-mediated aggregation of Aβ, further studies are required to elucidate the precise mechanism responsible for this effect.

Previous reports have stated that insulin/insulin-like growth factor type 1 (IGF-1) signaling is disturbed in AD patients [11]. Costantini et al. reported that IGF-1 signaling increased β-secretase, but not α-secretase, activity thereby enhancing Aβ production [28]. Moreover, the suppression of insulin signaling was reported to lead to the hyperphosphorylation of tau, another hallmark of AD, through the phosphorylation of glycogen synthase kinase (GSK)-3β [29]. Meanwhile, Cohen et al. suggested that IGF-1 resistance protects against Aβ-induced neurotoxicity by shifting from highly toxic low-weight molecular oligomers to low toxicity high-weight molecular assemblies [30]. These opposing effects might originate from the different phosphorylation pathways of the insulin/IGF-1 receptors and GSK-3β. Recently, impaired IGF-1/IR substrate 2 (IRS-2) signaling ameliorated some of Aβ-related phenotypes using the double mutant mice with Tg2576 (IRS-2 null [31,32], neuronal IGF-1 receptor null, and neuronal IR null [31]). These findings suggest roles for insulin/IGF-1 signaling and the antioxidant system in Aβ metabolism and clearance.

In conclusion, we found that insulin resistance does not accelerate AD symptoms such as amyloid deposition and memory decline. The molecular mechanism of the P1195L-meditated alleviation of Aβ deposition remains to be investigated.

Acknowledgments

This research was supported in part by the Program for the Promotion of Basic Research Activities for Innovative Biosciences (T.Shim) and Grants-in-Aid for Scientific Research (B) (No. 20390085 to T. Shir.), (C) (No. 20500641 to T. Shim.), (A) (No. 21248015 to K.I.), and (C) (No. 22603006 to K.M.) and the Promotion of Science for Young Scientists (No. 19.0403 to K.M.) from the Ministry of Education, Culture, Sports, Science, and Technology of the Japanese Government. We also thank Yoshihiro Noda, Eiko Moriizumi, Chizuru Tsuda, Shuichi Shibuya, Toshihiko Toda, Riya Takano, and Daichi Morikawa of Tokyo Metropolitan Institute of Gerontology for providing technical assistance.

Appendix A. Supplementary data

Supplementary data associated with this article can be found, in the online version, at doi:10.1016/j.bbrc.2011.04.101.

References

[1] G.G. Glenner, C.W. Wong, Alzheimer's disease: Initial report of the purification and characterization of a novel cerebrovascular amyloid protein, Biochem. Biophys. Res. Commun. 120 (1984) 885–890.
[2] C.L. Masters, G. Simms, N.A. Weinman, G. Multhaup, B.L. McDonald, K. Beyreuther, Amyloid plaque core protein in Alzheimer disease and Down syndrome, Proc. Natl. Acad. Sci. USA 82 (1985) 4245–4249.
[3] C. Haass, D.J. Selkoe, Soluble protein oligomers in neurodegeneration: lessons from the Alzheimer's amyloid β-peptide, Nat. Rev. Mol. Cell Biol. 8 (2007) 101–112.
[4] R. Roychaudhuri, M. Yang, M.M. Hoshi, D.B. Teplow, Amyloid β-protein assembly and Alzheimer disease, J. Biol. Chem. 284 (2009) 4749–4753.
[5] T. Gomez-Isla, R. Hollister, H. West, S. Mui, J.H. Growdon, R.C. Petersen, J.E. Parisi, B.T. Hyman, Neuronal loss correlates with but exceeds neurofibrillary tangles in Alzheimer's disease, Ann. Neurol. 41 (1997) 17–24.
[6] M. Meyer-Luehmann, T.L. Spires-Jones, C. Prada, M. Garcia-Alloza, A. De Calignon, A. Rozkalne, J. Koenigsknecht-Talboo, D.M. Holtzman, B.J. Bacskai, B.T. Hyman, Rapid appearance and local toxicity of amyloid-β plaques in a mouse model of Alzheimer's disease, Nature 451 (2008) 720–724.
[7] K.J. Barnham, C.L. Masters, A.I. Bush, Neurodegenerative diseases and oxidative stress, Nat. Rev. Drug Discov. 3 (2004) 205–214.
[8] K. Murakami, Y. Masuda, T. Shirasawa, T. Shimizu, K. Irie, The turn formation at positions 22 and 23 in the 42-mer amyloid β peptide: the emerging role in the pathogenesis of Alzheimer's disease, Geriatr. Gerontol. Int. 10 (2010) S169–179.
[9] P.A. Maher, D.R. Schubert, Metabolic links between diabetes and Alzheimer's disease, Expert. Rev. Neurother. 9 (2009) 617–630.
[10] B.J. Goldstein, Insulin resistance as the core defect in type 2 diabetes mellitus, Am. J. Cardiol. 90 (2002) 3G–10G.
[11] L. Frolich, D. Blum-Degen, P. Riederer, S. Hoyer, A disturbance in the neuronal insulin receptor signal transduction in sporadic Alzheimer's disease, Ann. NY Acad. Sci. 893 (1999) 290–293.
[12] M.N. Haan, Therapy insight: type 2 diabetes mellitus and the risk of late-onset Alzheimer's disease, Nat. Clin. Pract. Neurol. 2 (2006) 159–166.
[13] M. Townsend, T. Mehta, D.J. Selkoe, Soluble Aβ inhibits specific signal transduction cascades common to the insulin receptor pathway, J. Biol. Chem. 282 (2007) 33305–33312.
[14] L. Zhao, B. Teter, T. Morihara, G.P. Lim, S.S. Ambegaokar, O.J. Ubeda, S.A. Frautschy, G.M. Cole, Insulin-degrading enzyme as a downstream target of insulin receptor signaling cascade: implications for Alzheimer's disease intervention, J. Neurosci. 24 (2004) 11120–11126.
[15] T. Baba, T. Shimizu, Y. Suzuki, M. Ogawara, K. Isono, H. Koseki, H. Kurosawa, T. Shirasawa, Estrogen, insulin, and dietary signals cooperatively regulate longevity signals to enhance resistance to oxidative stress in mice, J. Biol. Chem. 280 (2005) 16417–16426.
[16] L. Mucke, E. Masliah, G.Q. Yu, M. Mallory, E.M. Rockenstein, G. Tatsuno, K. Hu, D. Kholodenko, K. Johnson-Wood, L. McConlogue, High-level neuronal expression of Aβ1–42 in wild-type human amyloid protein precursor transgenic mice. Synaptotoxicity without plaque formation, J. Neurosci. 20 (2000) 4050–4058.
[17] N. Murata, K. Murakami, Y. Ozawa, N. Kinoshita, K. Irie, T. Shirasawa, T. Shimizu, Silymarin attenuated the amyloid β plaque burden and improved behavioral abnormalities in an Alzheimer's disease mouse model, Biosci. Biotechnol. Biochem. 74 (2010) 2299–2306.
[18] K. Murakami, N. Murata, Y. Ozawa, N. Kinoshita, K. Irie, T. Shirasawa, T. Shimizu, Vitamin C restores behavioral deficits and Aβ oligomerization without affecting plaque formation in a mouse model of Alzheimer's disease, J. Alzheimers Dis. 26 (2011), in press.
[19] T. Toda, Y. Noda, G. Ito, M. Maeda, T. Shimizu, Presenilin-2 mutation causes early amyloid accumulation and memory impairment in a transgenic mouse model of Alzheimer's disease, J. Biomed. Biotech. 2011 (2011) 617974.
[20] M.J. Callahan, W.J. Lipinski, F. Bian, R.A. Durham, A. Pack, L.C. Walker, Augmented senile plaque load in aged female β-amyloid precursor protein-transgenic mice, Am. J. Pathol. 158 (2001) 1173–1177.
[21] R.O. Sanchez-Mejia, J.W. Newman, S. Toh, G.Q. Yu, Y. Zhou, B. Halabisky, M. Cisse, K. Scearce-Levie, I.H. Cheng, L. Gan, J.J. Palop, J.V. Bonventre, L. Mucke, Phospholipase A2 reduction ameliorates cognitive deficits in a mouse model of Alzheimer's disease, Nat. Neurosci. 11 (2008) 1311–1318.
[22] P.I. Moreira, M.A. Smith, X. Zhu, A. Nunomura, R.J. Castellani, G. Perry, Oxidative stress and neurodegeneration, Ann. NY Acad. Sci. 1043 (2005) 545–552.
[23] J.A. Luchsinger, M.X. Tang, S. Shea, R. Mayeux, Hyperinsulinemia and risk of Alzheimer disease, Neurology 63 (2004) 1187–1192.
[24] K.D. Kimura, H.A. Tissenbaum, Y. Liu, G. Ruvkun, Daf-2 an insulin receptor-like gene that regulates longevity and diapause in *Caenorhabditis elegans*, Science 277 (1997) 942–946.
[25] S. Hekimi, Genetics and the specificity of the aging process, Science 299 (2003) 1351–1354.
[26] C. Curtis, G.N. Landis, D. Folk, N.B. Wehr, N. Hoe, M. Waskar, D. Abdueva, D. Skvortsov, D. Ford, A. Luu, A. Badrinath, R.L. Levine, T.J. Bradley, S. Tavare, J. Tower, Transcriptional profiling of mnsod-mediated lifespan extension in drosophila reveals a species-general network of aging and metabolic genes, Genome Biol. 8 (2007) R262.
[27] V. Chavez, A. Mohri-Shiomi, A. Maadani, L.A. Vega, D.A. Garsin, Oxidative stress enzymes are required for daf-16-mediated immunity due to generation of reactive oxygen species by *Caenorhabditis elegans*, Genetics 176 (2007) 1567–1577.
[28] C. Costantini, H. Scrable, L. Puglielli, An aging pathway controls the Trka to p75 NTR receptor switch and amyloid β-peptide generation, EMBO J. 25 (2006) 1997–2006.
[29] M. Hong, V.M. Lee, Insulin and insulin-like growth factor-1 regulate tau phosphorylation in cultured human neurons, J. Biol. Chem. 272 (1997) 19547–19553.
[30] E. Cohen, J. Bieschke, R.M. Perciavalle, J.W. Kelly, A. Dillin, Opposing activities protect against age-onset proteotoxicity, Science 313 (2006) 1604–1610.
[31] S. Freude, M.M. Hettich, C. Schumann, O. Stohr, L. Koch, C. Kohler, M. Udelhoven, U. Leeser, M. Muller, N. Kubota, T. Kadowaki, W. Krone, H. Schroder, J.C. Bruning, M. Schubert, Neuronal IGF-1 resistance reduces Aβ accumulation and protects against premature death in a model of Alzheimer's disease, FASEB J. 23 (2009) 3315–3324.
[32] R. Killick, G. Scales, K. Leroy, M. Causevic, C. Hooper, E.E. Irvine, A.I. Choudhury, L. Drinkwater, F. Kerr, H. Al-Qassab, J. Stephenson, Z. Yilmaz, K.P. Giese, J.P. Brion, D.J. Withers, S. Lovestone, Deletion of Irs2 reduces amyloid deposition and rescues behavioural deficits in APP transgenic mice, Biochem. Biophys. Res. Commun. 386 (2009) 257–262.